Aalto University

Aaltodoc
OPEN ACCESS

This is an electronic reprint of the original article.
This reprint may differ from the original in pagination and typographic detail.

Author(s): Puska, M. J. & Pöykkö, S. & Pesola, M. & Nieminen, Risto M.

Title: Convergence of supercell calculations for point defects in semiconductors: Vacancy in silicon

Year: 1998

Version: Final published version

Please cite the original version:

Puska, M. J. & Pöykkö, S. & Pesola, M. & Nieminen, Risto M. 1998. Convergence of supercell calculations for point defects in semiconductors: Vacancy in silicon. Physical Review B. Volume 58, Issue 3. 1318-1325. ISSN 1550-235X (electronic). DOI: 10.1103/physrevb.58.1318.

Rights: © 1998 American Physical Society (APS). This is the accepted version of the following article: Puska, M. J. & Pöykkö, S. & Pesola, M. & Nieminen, Risto M. 1998. Convergence of supercell calculations for point defects in semiconductors: Vacancy in silicon. Physical Review B. Volume 58, Issue 3. 1318-1325. ISSN 1550-235X (electronic). DOI: 10.1103/physrevb.58.1318, which has been published in final form at http://journals.aps.org/prb/abstract/10.1103/PhysRevB.58.1318.

All material supplied via Aaltodoc is protected by copyright and other intellectual property rights, and duplication or sale of all or part of any of the repository collections is not permitted, except that material may be duplicated by you for your research use or educational purposes in electronic or print form. You must obtain permission for any other use. Electronic or print copies may not be offered, whether for sale or otherwise to anyone who is not an authorised user.

Convergence of supercell calculations for point defects in semiconductors: Vacancy in silicon

M. J. Puska, S. Pöykkö, M. Pesola, and R. M. Nieminen
Laboratory of Physics, Helsinki University of Technology, P.O. Box 1100, FIN-02015 HUT, Finland
(Received 10 February 1998)

The convergence of first-principles supercell calculations for defects in semiconductors is studied with the vacancy in bulk Si as a test case. The ionic relaxations, defect formation energies, and ionization levels are calculated for supercell sizes of up to 216 atomic sites using several **k**-point meshes in the Brillouin-zone integrations. The energy dispersion, inherent for the deep defect states in the supercell approximation, and the long range of the ionic relaxations are shown to postpone the convergence so that conclusive results for the physical properties cannot be obtained before the supercell size is of the order of 128–216 atomic sites. [S0163-1829(98)05627-6]

I. INTRODUCTION

First-principles electronic structure calculations based on the density-functional theory within the local-density approximation (LDA) for the electron exchange-correlation energy[1] are often used to study low-concentration defects (of the order of one defect per million lattice sites) in semiconductors, metals, and insulators. Typically, the aim of the calculations is to describe isolated defects in an otherwise perfect crystal lattice. In principle, the Green's-function methods[2] treat this limit exactly, but are not very practical for the large embedded clusters necessary to incorporate the long-range ionic relaxations. In the popular supercell approximation one repeats periodically a finite unit cell containing the defect desired plus neighboring host atoms. The periodicity of the ensuing superlattice enables the use of powerful calculation methods designed originally for perfect bulk lattices. One of them is the pseudopotential plane-wave method,[3] which also enables an accurate calculation of the forces affecting the ions and thereby the optimization of the ionic structure around the defect. The supercell approximation has obvious drawbacks in terms of the interactions between the defect and its periodic replicas. If the defect-defect distance is not large enough the electronic structure of an isolated defect is distorted because the deep levels in the band gap form energy bands with a finite dispersion and the localization of the deep level wave functions may change considerably. In the worst case the deep level may end up [at least for some **k** points in the superlattice Brillouin zone (BZ)] in the region of the bulk energy bands resulting in strong hybridization. The size of the supercell restricts also the ionic relaxation. The relaxation pattern is truncated midway between a defect and its nearest periodic replica. In the case of long-range ionic relaxations this cutoff may be reflected dramatically close to the defect, as will be demonstrated below.

The vacancy in bulk Si can be considered as the simplest example of a point defect in a semiconductor lattice. Vacancies in Si play an important role, e.g., in self- and impurity diffusion and therefore the knowledge of their ionic and electronic structures is of utmost importance. Experimentally, vacancies in Si have successfully been monitored using the electron paramagnetic resonance technique (EPR), the electron-nuclear double resonance (ENDOR), and the deep-level transient spectroscopy (DLTS).[4] EPR and ENDOR give the symmetries and spatial distributions of the highest unpaired localized electron state. DLTS and EPR give information about the ionization levels, i.e., about the values of the electron chemical potential at which the defect changes its charge state. Positron lifetime measurements have given information about the open volume changes for the vacancy-phosphorus pair in Si when the charge state of the defect changes.[6] Also DLTS has been used for this purpose.[7]

Watkins has described the electronic and ionic structure of the vacancy in Si on the basis of the linear combination of atomic orbitals (LCAO) model.[4] When a Si atom is removed from the lattice, four dangling bonds, directed towards the center of the vacancy, are formed. These dangling bonds hybridize so that their totally symmetric combination, an s-type state, lies in energy within the bulk valence band. Three different combinations with nodal planes are p type and they form deep levels in the energy gap. In the doubly positive charge state of the defect the deep levels are empty and the ionic relaxation preserves the T_d-point symmetry of the perfect lattice. In the singly positive and neutral charge states one of the deep levels is occupied by one and two electrons, respectively. The Jahn-Teller effect lowers the point symmetry to D_{2d} and breaks the degeneracy of the deep levels. This symmetry is deduced from the EPR measurement.[5] Actually, the introduction of the second electron to the deep level results in a strong ionic relaxation and a lowering of the total energy, overcoming the Coulombic repulsion between the localized electrons. Therefore, it is energetically favorable that the charge state changes directly from the doubly positive to the neutral one. This is the famous negative-effective-U effect first predicted for the Si vacancy by Baraff *et al.*[8] and experimentally confirmed by Watkins and Troxel.[9] For the negative and doubly negative charge states the symmetry is further lowered and the point symmetry derived from the EPR (Ref. 5) and ENDOR (Ref. 10) measurements is C_{2v}.

In spite of its obvious simplicity, the vacancy in Si is a most challenging application for first-principles electronic structure calculations, although this fact has not always been fully appreciated. Sugino and Oshiyama[11] realized the difficulties of the supercell calculations when describing the

0163-1829/98/58(3)/1318(8)/$15.00 PRB 58 © 1998 The American Physical Society

highest occupied electronic state of the Si vacancy in the negative charge state. Difficulties arise especially when one searches for the ionic positions around the defect without any (point) symmetry restrictions. The electronic and ionic structures are strongly coupled together, which is most clearly seen in a spectrum of different ionic relaxation patterns obtained as the approximations of the calculation vary. The early Green's-function calculations[12] predicted that the ions surrounding the vacancy in the neutral charge state relax *outwards* from the center of the vacancy. The physics behind this kind of pattern was explained to be the creation of sp^2-type hybridization for the ions surrounding the vacancy. Later calculations employing the supercell approximation within the plane-wave[13,14] or tight-binding[15] schemes converged with an *inward* relaxation (of nearest-neighbor atoms), having a component lowering the symmetry from T_d to the pairing-type D_{2d} point symmetry. This was the result also in a recent cluster calculation for the Si vacancy.[16] However, the results can be sensitive to the computational details and also more complicated relaxation patterns have been found.[17] Besides the ionic relaxations, also the calculated vacancy formation energy and the ionization levels show remarkably scattered results between different works.

In this work we study systematically the convergence of the LDA supercell calculations in the case of the vacancy in silicon. Supercell sizes of up to 216 atomic sites are employed and the Brillouin zone is sampled using several **k**-point sets. These kinds of calculations have become feasible only during the last years with the massively parallel supercomputers and electronic-structure codes especially designed for them.[18,19] For Si we have used separable[20] first-principles norm-conserving pseudopotentials.[21,22] The nonlinear core-valence corrections[23] are used to account for the overlap of the core and the valence-electron charges. The pseudopotential has been carefully tested, in particular it has been confirmed to be free of unphysical ghost states[24] using the analysis by Gonze *et al.*[25] The valence electron structures have been solved within the LDA (Ref. 26) and the plane-wave basis set with a high cutoff energy of 15 Ry. Using the unit cell of two atoms and increasing the number of **k** points the equilibrium lattice constant of bulk Si converges to 5.39 Å. This is slightly less than the experimental value of 5.43 Å. The discrepancy is typical for LDA calculations. Our calculation gives for the energy band gap the value of 0.47 eV. The underestimation with respect to the experimental value of ~1.2 eV is also typical for LDA calculations. The supercells used for the vacancy calculations and the geometric properties of the corresponding superlattices are given in Table I.

In all our defect calculations, unless otherwise stated, all the atoms in the supercell have been allowed to move without any symmetry restrictions. In the beginning of each relaxation atomic positions have been slightly randomized in order to remove any spurious symmetries. In order to avoid artificial stresses the lattice constant for a defect calculation should be obtained from a bulk calculation using the same density of **k** points as in the defect calculation. The typical variations of the lattice constant are in our calculations small, of the order of 0.2%. The ensuing variations in ionic relaxation patterns and in total energies are not significant. This we have tested with the doubly positive vacancy described by the supercell of 64 atomic sites. The calculations indicate that changes up to 1% in the lattice constant do not significantly affect the results. Therefore we have used, for simplicity, the same lattice constant of 5.39 Å in all of our subsequent calculations.

TABLE I. Details of the supercells used. The size of the supercell (N), the type of the superlattice, and the smallest distance (D) from a site in a supercell to its periodic image are given.

N	Superlattice	D (in units of the superlattice constant a)
32	bcc	1.732
64	sc	2.000
128	fcc	2.828
216	sc	3.000

The organization of the paper is as follows: In Sec. II a survey of the approximations used in the Brillouin-zone summations is given. In Secs. III and IV we discuss the results, and compare them with both experiment and the most recent theoretical calculations. Section V summarizes the results and gives the main conclusions.

II. BRILLOUIN-ZONE SAMPLING

For a perfect lattice the convergence of the electronic properties can be achieved by increasing the number of **k** points in the Brillouin zone, or, alternatively, the product of the number of atoms in the calculational unit cell and the number of **k** points. In conventional electronic-structure calculations the increase of the number of **k** points is much more economical than the increase of the number of atoms: the CPU time needed scales linearly with the former but is proportional to the cube of the latter number. In the supercell calculations for defects one would also like to use as small supercells as possible but now the convergence is a more subtle question due to the spurious defect-defect interactions in the superlattice. Although the description of the properties of the underlying perfect lattice can be improved just by increasing the number of **k** points, isolated defect properties cannot be obtained until the unit cell is large enough. For defects in metals already quite small supercells may give well converged results if the number of **k** points is large enough.[27] For defects in semiconductors the situation is more difficult. This is because the defects in semiconductors involve localized states and the description of these states, as will be shown below, is not straightforwardly improved as the number of **k** points increases, i.e., the detailed choice of the **k**-point sampling for the BZ integration may strongly affect the convergence. However, in most defect calculations BZ-sampling methods developed to describe bulk lattices are used.

The simplest scheme to sample the BZ in supercell calculations is to use the Γ point only. When the size of the supercell increases the wave functions calculated correspond to several **k** points of the underlying perfect bulk lattice so that the perfect lattice **k** space is evenly sampled. This scheme offers also saving in computer resources because the wave functions are purely real. In order to improve the de-

scription of the wave functions, especially that of the delocalized bulklike states, and the description of the electron density, it is beneficial to use **k** points other than the Γ point.[28] Thereby also components with wavelengths longer than the supercell lattice constant are included in the plane-wave expansions of the density and wave functions. This idea leads to the so-called special **k**-point schemes,[29–32] which are widely used to sample the BZ also in defect calculations.

Recently, Makov *et al.*[33] introduced a scheme to choose **k** points for the supercell defect calculations so that the defect-defect interactions are minimized in the total defect energy. They justified the different choices by a tight-binding model. For example, the **k**-point set minimizing the defect-defect interactions between the nearest-neighbor cells in the case of a simple cubic superlattice without any symmetry in the supercell consists of the Γ and the L points [L is the corner point $(\frac{1}{2},\frac{1}{2},\frac{1}{2})(2\pi/a)$ of the BZ of the superlattice with the lattice constant a]. At the L point the wave functions are purely real as in the Γ point, but they change sign between the adjacent cells. The use of these two **k** points was recommended also by Korhonen *et al.*[34] in the context of localized positron states at lattice defects. Korhonen *et al.* justified the recommendation by real-space arguments. Recently, also Chadi *et al.*[35] have used these two **k** points in defect calculations.

In our calculations we have employed several **k**-point sets to sample the BZ in order to systematically test the effects of the sampling. The simplest one uses the Γ point only. The 2^3 **k**-point meshes are those by Monkhorst and Pack (MP) (Ref. 31) (eight points in the BZ). In the case of the supercell with 64 atomic sites we have also employed the 3^3 MP **k**-point mesh (27 points in the BZ). The 3^3 MP mesh contains the Γ point whereas the 2^3 MP mesh samples the Brillouin zone ignoring the Γ point. The **k**-point meshes recommended by Makov *et al.*[33] have been used for supercells with 32 [one **k**-point, $(\frac{1}{4},\frac{1}{4},\frac{1}{4})(2\pi/a)$] and 64 (the Γ and L points) atomic sites.

III. NEUTRAL Si VACANCY

A. Vacancy formation energy

The formation energy of a vacancy in Si in the charge state Q is calculated in the supercell approximation as

$$E_Q^v(\mu_e)=E_Q^{N-1}+Q(\mu_e+E_v)-\frac{N-1}{N}E^N, \qquad (3.1)$$

where E^N is the total energy of the perfect lattice supercell with N atoms and E_Q^{N-1} is the total energy of the supercell containing one vacancy. The electron chemical potential μ_e in Eq. (3.1) gives the position of the Fermi level in the band gap relative to the top of the valence band E_v. Average potential correction has been employed in the calculation of the position of the valence-band maximum in the defect supercell.[36–38] We use a neutralizing uniform background charge in order to avoid long-range Coulomb interactions between the supercells. When applying Eq. (3.1) we use in the defect and perfect lattice calculations supercells of the same volume and we also use the same **k**-point samplings. In

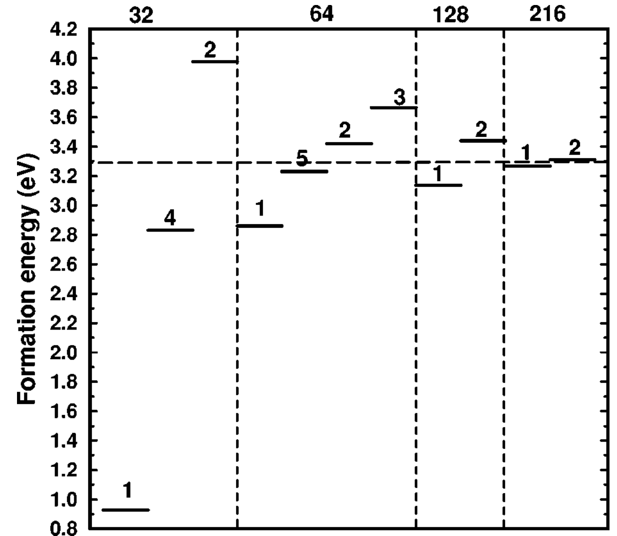

FIG. 1. Formation energy of the neutral vacancy in Si. The supercell size used is given on the top of each panel and the **k**-point set used to sample the Brillouin zone is indicated as numbers; $1=\Gamma$, $2=2^3$, $3=3^3$, $4=(\frac{1}{4},\frac{1}{4},\frac{1}{4})$, and $5=\Gamma+L$.

this way some systematic errors, especially those arising from bulk components, cancel out in the calculated energy differences.

The neutral vacancy formation energies obtained with different supercell sizes and **k**-point samplings after relaxing all the ions without any symmetry restriction are given in Fig. 1. The vacancy formation energies calculated using the Γ-point sampling increase strongly and systematically as the size of the supercell increases. The Γ-point sampling contains the (electronic) interactions between neighboring defects in the superlattice as discussed by Makov *et al.*[33] In the Γ-point sampling these interactions are *attractive* and they decay off as the size of the supercell increases. The 2^3 MP mesh gives in the case of small supercells formation energies that are larger than the best converged value reflecting *repulsive* components of the defect-defect interactions. However, this sampling seems to lead to a faster convergence than the Γ point, indicating that some of the nearest-neighbor defect-defect interactions are canceled. Finally, it is interesting to see that the calculations using the **k**-point samplings recommended by Makov *et al.* seem to result in a fast convergence of the formation energy. This happens in spite of the fact that the relaxation pattern of the vacancy has not yet converged. Thus, from the energetical point of view the minimization of the (electronic) defect-defect interactions seems to be more important than the detailed positions of the ions.

In order to get an idea of the energy surfaces in the space spanned by the position coordinates of the ions we have taken the ionic positions in the supercell with 64 atomic sites calculated using a given **k**-point sampling and repeated the calculation with other **k**-point samplings, keeping the ionic positions fixed. The total-energy differences relative to the original calculation with self-consistently relaxed ionic positions are given in Table II. Firstly, the matrix formed shows that the self-consistent ionic positions always give the smallest total energy supporting our contention that we have found in each self-consistent calculation the global energy minimum with respect to the ionic positions. Secondly, it is

TABLE II. Calculated total-energy differences between the most stable structures for a neutral vacancy in Si and the structures obtained using different **k**-point sets. In these calculations a supercell of 64 atomic sites has been employed. Energies are given in eV.

Ionic structure	**k**-point set Γ	$\Gamma+L$	2^3	3^3
Γ	0.00	0.18	0.88	0.75
$\Gamma+L$	0.13	0.00	0.13	0.03
2^3	0.34	0.27	0.00	~0.00
3^3	0.18	0.04	0.06	0.00

amazing that the energy differences between the ionic configuration with a relatively large outward relaxation obtained with the self-consistent Γ-point calculation and those with a large inward relaxation from the other **k**-point samplings (columns in Table II) are quite small. In the case of the Γ-point sampling for the electronic structure the energy differences between the ionic structures calculated employing different **k**-point sets are only a few tenths of eV (the first column in Table II). This means a flat energy surface implying that the finding of the energy minimum requires the iteration of the forces acting on the ions very close to zero. That requires, in turn, a huge amount of iteration steps for the ionic positions. We have iterated atomic positions until the largest remaining force component acting on any ion is less than 3×10^{-5} Ry/a_0.

B. Ionic relaxation

We have studied in detail the ionic relaxation pattern around the neutral vacancy in Si, both the resulting point symmetry and the magnitude of the ionic movements with respect to the ideal lattice positions. Table III gives the results. The distances between the four nearest-neighbor ions of the vacancy as well as the resulting relaxation volumes with respect to the ideal vacancy are given. The point-symmetry groups are deduced from the nearest-neighbor distances. In many cases, there is a small numerical noise component in the distances and an ensuing slight indefiniteness in the symmetry group. The flatness of the total-energy surface in the space of ionic coordinates (see Table II) explains this noise and partly the scatter in the relaxation patterns between different calculations (see Table III).

If the vacancy conserves the T_d-point symmetry of the ideal vacancy, all the six lengths in Table III are equal. The D_{2d}-point symmetry is signaled by four equal, longer distances and two equal, shorter distances. If four of the distances are equal and from the remaining two distances one is longer than the other the point symmetry is C_{2v}. According to Table III the final D_{2d} -point symmetry, which is in agreement with the present common opinion,[4] is obtained consistently only for the largest supercell of 216 atomic sites. In the case of the supercell with 128 atomic sites the Γ-point sampling gives the D_{2d} symmetry whereas for the supercell of 64 atomic sites this symmetry is obtained with the largest 3^3 sampling, which contains the Γ point. It is striking that the simulation with the supercell of 64 sites and the Γ-point sampling gives a strong outward relaxation of the nearest-neighbor ions and the point symmetry of C_{2v}. The deviation from the other calculations illustrates clearly the difficulties encountered in the supercell calculations for the vacancy in Si.

Some of the scatter in the results of Table III can be understood on the basis of the energy dispersion of the vacancy-induced deep levels. Because the deep-level wave functions are of p type their energy dispersion resembles that of the top of the valence band: moving away from the Γ point the possible threefold degeneracy is broken and the energy eigenvalues are lowered. If the supercell consists of 64 atomic sites our electronic structure calculations give for the energy dispersion the estimate of 0.7 eV. For the supercell of 216 atomic sites the corresponding estimate is 0.2 eV. Thus for the small supercell sizes the energy dispersion is even larger than the LDA band gap. This may lead to the

TABLE III. Distances between the ions neighboring the neutral vacancy in Si. In the perfect crystal, all distances are equal to 3.81 Å. The relative volume change $(V-V_0)/V_0$ and the resulting point symmetry group when the ions relax from their ideal lattice positions are also given. V and V_0 are calculated as the volumes of the tetrahedra formed by the four nearest-neighbor ions of the relaxed and the ideal vacancy, respectively. E^v is the vacancy-formation energy defined in Eq. (1). Distances are given in Å and energies in eV.

Supercell	BZ sampling	Distance number (1)–(2)	(3)	(4)	(5)	(6)	$100(V-V_0)/V_0$	Symmetry	E^v
216	2^3	3.38	3.38	3.36	2.96	2.90	−41.4	$\sim D_{2d}$	3.31
216	Γ	3.39	3.39	3.39	2.89	2.89	−42.4	D_{2d}	3.27
128	2^3	3.43	3.43	3.41	3.41	3.41	−27.6	$\sim T_d$	3.44
128	Γ	3.55	3.55	3.55	3.09	3.00	−33.2	$\sim D_{2d}$	3.14
64	3^3	3.47	3.47	3.47	3.16	3.15	−32.4	$\sim D_{2d}$	3.67
64	2^3	3.40	3.40	3.40	3.40	3.40	−29.0	T_d	3.42
64	$\Gamma+L$	3.57	3.57	3.57	3.34	2.96	−29.5	C_{2v}	3.23
64	Γ	4.16	4.07	4.07	4.83	3.06	+11.7	$\sim C_{2v}$	2.86
32	2^3	3.61	3.61	3.61	3.52	3.52	−17.4	$\sim T_d$	3.98
32	$(\frac{1}{4},\frac{1}{4},\frac{1}{4})$	3.33	3.33	3.20	3.20	3.20	−37.2	C_{3v}	2.83
32	Γ	4.27	3.99	3.99	2.48	2.47	−44.1	σ_{1v}	0.93

hybridization of the deep-level states with the valence-band states, and the delocalized character of the wave functions can be strongly enhanced.

For the Γ point the deep-level energy eigenvalue falls into the band gap. Therefore, the Γ-point calculation for the supercell of 128 atomic sites can give the correct D_{2d} symmetry. In contrast, the calculations employing the Monkhorst-Pack 2^3 **k**-point mesh conserve the T_d symmetry up to the supercell of 128 atomic sites. In comparison with the Γ-point calculation for the T_d-symmetric vacancy, the triply degenerate deep state is split at each **k** point into a nondegenerate and a doubly degenerate state. The energy dispersion of the nondegenerate state is so strong that its eigenenergy falls into the valence band. The delocalized character of the hybridized states is then seen as the conservation of the T_d symmetry.

The relative relaxation volume $(V-V_0)/V_0$ shows a tendency to increase when increasing the size of the supercell (compare the numbers with the similar **k**-point samplings for the supercells of 128 and 216 sites). The tendency is due to the completion of the long-range ionic relaxation pattern: when the size of the supercell increases, ions neighboring the vacancy can move more from their ideal lattice positions. The dependence of the relaxation amplitude on the supercell size can be compared with the results by Öğüt *et al.*[16] They solved the electronic and ionic structures of the Si vacancy by the cluster method so that the surface Si ions of the clusters were fixed at the perfect bulk positions. They found also that the inward relaxation of the nearest-neighbor ions of the vacancy increases when the size of the cluster increases. The convergence occurred when there were about 100 Si atoms in the cluster.

According to Table III the calculations for the supercells of 32 and 64 atomic sites by employing the **k** points recommended by Makov *et al.*[33] do not result in the correct D_{2d} symmetry. However, the relaxation of the nearest neighbor ions is in both calculations into the correct direction, i.e., inwards.

C. Comparison with previous results

Our results can be compared with several other recent supercell calculations for the neutral vacancy in silicon. Below we discuss some of them in chronological order. The comparison is hindered by the different types of pseudopotentials and plane-wave cutoff energies used, but nevertheless quantitative trends in the results with respect to the supercell size and the **k**-point sampling can be seen.

Blöchl *et al.*[39] used the supercell of 64 atomic sites and sampled the BZ with up to 27 **k** points ($=3^3$ MP mesh). Their rather high value for the formation energy, 4.1 eV, is consistent with our finding that the 3^3 BZ sampling gives the highest formation energy of the different **k**-point sets used for the supercell of 64 atomic sites.

Virkkunen *et al.*[17] calculated the electronic and ionic structures of the Si vacancy using the supercell of 64 atomic sites and the Γ point for the BZ sampling. Using the pseudopotential with *s* and *p* nonlocality the neutral vacancy relaxed according to the C_{3v}-point symmetry so that one of the nearest-neighbor atoms moved strongly to the open [111] direction. The formation energy was found to be 2.8 eV. This value as well as the strong outward relaxation, although different in details, are in good agreement with our present calculation.

Seong and Lewis[14] calculated the electronic and ionic structure of the Si vacancy using the supercell of 64 atomic sites and the Γ point for the BZ sampling. They found the D_{2d}-point symmetry and an inward relaxation so that the relative volume change of the vacancy is -35%. For the vacancy-formation energy they obtained the value of 3.29 eV. The result contradicts our final fully converged results for this supercell and BZ sampling with a large outward relaxation of the nearest-neighbor ions. However, our calculations converged first very close to the D_{2d} symmetry with an inward relaxation and only several further iterations changed very slowly the relaxation to the outward direction and the symmetry to C_{2v}. Our final vacancy-formation energy with the 64 atomic-site supercell and the Γ-point sampling is 2.86 eV, which is lower than 3.29 eV obtained by Seong and Lewis.[14] Using the numbers of Table II one can estimate that our Γ-point value with the inward relaxation of the order of -35% in volume would be around 3.0–3.2 eV.

Ramamoorthy and Pantelides[40] calculated the vacancy-formation energy using a supercell of 32 atomic sites and two special **k** points.[30] They obtained the value of 3.78 eV, which is not far away from our value of 3.98 eV calculated for this supercell size with the 2^3 MP **k**-point mesh.

Pankratov *et al.*[41] used the supercell with 64 atomic sites and eight special **k**-points (2^3 MP mesh). They obtained the vacancy-formation energy of 3.6 eV, which is only slightly higher than our value of 3.42 eV calculated for this supercell size with the 2^3 MP mesh.

Zywietz *et al.*[42] studied the occurrence of the Jahn-Teller distortion in the neutral Si vacancy by supercells of up to 128 atomic sites and using several **k**-point samplings. They restricted the relaxations to obey the T_d, D_{2d}, or C_{3v} symmetry. The formation energies they obtained with the Γ point as well as with the 2^3 and 3^3 meshes are in agreement with our values within an accuracy of the order of 0.1 eV. It is also remarkable that their calculations with a given supercell size and **k**-point sampling gave for the vacancies with different symmetries nearly the same total energies. This reflects, as discussed in the context of Table II, the difficulty of finding the ground-state ionic configuration.

IV. CHARGED Si VACANCIES

We have also made calculations for the charged states of the vacancy in Si. The ionic structures of the charged vacancies, when using different computational approximations, are given in Table IV. The doubly positive charge state, which has no electrons in the deep levels, shows the expected T_d-point symmetry. However, the size of the supercell is seen to have a remarkable influence. For the supercells with 128 or less atomic sites the nearest-neighbor ions relax slightly outwards irrespective of the **k**-point sampling. But increasing the supercell to 216 atomic sites the nearest-neighbor ions relax suddenly strongly inwards. This change in the relaxation pattern is in agreement with the results of the recent cluster calculations by Öğüt *et al.*[16] It reflects the fact that the vacancy-induced ionic distortions in Si propagate preferably in the [110] zigzag directions.[15] The defect-

TABLE IV. Same as Table III but for charged vacancies in Si.

Charge state Q	Supercell	BZ sampling	Distance number (1)–(2)	(3)	(4)	(5)	(6)	$100(V-V_0)/V_0$	Symmetry	$E^v_Q(\mu_e=0)$
2+	216	Γ	3.45	3.45	3.45	3.45	3.45	−26.1	T_d	3.01
2+	128	Γ	3.89	3.89	3.89	3.89	3.89	6.4	T_d	2.57
2+	64	3^3	3.85	3.85	3.84	3.84	3.84	2.6	$\sim T_d$	3.79
2+	64	2^3	3.85	3.85	3.84	3.84	3.84	2.6	$\sim T_d$	4.11
2+	64	$\Gamma+L$	3.92	3.92	3.92	3.92	3.92	8.7	T_d	2.45
2+	64	Γ	3.83	3.83	3.83	3.83	3.83	1.7	T_d	2.01
1+	216	Γ	3.38	3.39	3.37	3.03	2.98	−39.4	$\sim D_{2d}$	3.20
1+	128	Γ	3.76	3.76	3.76	3.68	3.63	−6.9	$\sim T_d$	2.89
1+	64	3^3	3.62	3.62	3.62	3.62	3.62	−14.3	T_d	3.62
1+	64	2^3	3.62	3.61	3.61	3.61	3.61	−14.8	T_d	3.72
1+	64	$\Gamma+L$	3.79	3.79	3.79	3.73	3.70	−3.8	$\sim T_d$	2.85
1+	64	Γ	3.74	3.74	3.74	3.73	3.69	−6.2	$\sim T_d$	2.51
1−	216	Γ	3.49	3.47	2.63	2.62	2.60	−55.0	$\sim D_{3d}$	3.88
1−	128	Γ	3.56	3.52	3.52	3.41	2.76	−33.4	$\sim C_{2v}$	3.53
1−	64	3^3	3.35	3.33	3.33	3.15	3.06	−37.9	$\sim C_{2v}$	4.07
1−	64	2^3	3.34	3.30	3.29	3.14	3.14	−37.7	$\sim D_{2d}$	3.68
1−	64	$\Gamma+L$	3.52	3.50	3.50	3.59	2.72	−26.6	$\sim C_{2v}$	3.85
1−	64	Γ	3.51	3.50	3.50	2.94	2.90	−38.2	$\sim D_{2d}$	3.56
2−	216	Γ	3.47	3.47	2.60	2.60	2.60	−51.9	D_{3d}	4.29
2−	128	Γ	3.56	3.46	3.46	3.32	2.68	−36.8	$\sim C_{2v}$	4.17
2−	64	3^3	3.31	3.07	3.07	3.06	3.06	−44.5	$\sim D_{2d}$	4.60
2−	64	2^3	3.31	3.07	3.07	3.06	3.06	−44.5	$\sim D_{2d}$	4.01
2−	64	$\Gamma+L$	3.46	3.40	3.39	3.55	2.62	−37.7	$\sim C_{2v}$	4.52
2−	64	Γ	3.49	3.48	3.47	2.79	2.75	−43.4	$\sim D_{2d}$	4.15

defect distance in the [110] direction is the same in the supercells with 64 and 128 atomic sites and the distance is too small to allow an inward relaxation. In going to the supercell of 216 atomic sites the defect-defect distance increases in the [110] direction by the factor of 1.5 and the relaxation pattern changes.

When the charge state of the vacancy is changed from doubly positive to singly positive its point symmetry is lowered from T_d towards D_{2d} for those supercell sizes and **k**-point samplings, that give a low-symmetry structure in the neutral-charge state. The symmetry patterns obtained are not as clear as in the neutral-charge state. The very strong symmetry-breaking relaxation mode seen in the neutral-charge state when calculating with the Γ-point sampling and the 64-atomic-site supercell is not seen in the singly positive charge state. The convergence of the ionic relaxation is similar to that for the doubly positive charge state: a supercell of 216 atomic sites is required to describe the long-range relaxation pattern. Then the point symmetry of the defect is D_{2d}, i.e., the one obtained in the EPR measurements.[5]

For the negative-charge states the convergence of the ionic relaxation with respect to supercell size and the **k**-point sampling is slower than for the neutral-charge state (see Tables III and IV). The results can be affected by the too narrow band gap of the LDA. The highest defect-induced level can be strongly hybridized with the conduction-band states. The highest-occupied electron states then have a wrong character and the ionic relaxation differs from what would be obtained with a larger band gap consistent with the experiments. Our calculations performed with the supercell of 216 atomic sites and the Γ-point sampling for the singly and doubly negative charge states converge to the D_{3d}-point symmetry. In this solution one of the nearest-neighbor ions of the vacancy has relaxed towards to the center of the vacancy so that a symmetric ''split vacancy'' results (see Fig. 2). The ion in the middle of the defect is bonded to six neighboring ions. In the doubly negative vacancy the highest electron state is doubly degenerate and it lies in the band gap. The state is fully occupied by four electrons so that there is no Jahn-Teller distortion, which would lower the D_{3d}-point symmetry. The highest occupied level is an e_g orbital resembling the corresponding orbital obtained in the LCAO model for an ideal divacancy.[43] The electron density of the fully occupied level is given in Fig. 2 showing that the density is localized in the six dangling bonds of the split vacancy. For the singly negative charge state a Jahn-Teller symmetry lowering should take place. According to our results in Table IV the amplitude of the symmetry lowering is small and the result is in disagreement with the EPR (Ref. 5) and ENDOR (Ref. 10) measurements indicating the C_{2v}-point symmetry for the singly negative vacancy.

Sugino and Oshiyama[11] made supercell calculations for the singly-negative vacancy in Si. First they obtained the ionic structure by using a supercell of 64 atomic sites and the 2^3 MP **k**-point mesh. The symmetry was found to be C_{2v}. Our calculation with the same supercell size and **k**-point sampling gives ionic relaxations similar in magnitude but different in symmetry. Using the ionic positions obtained with the small supercell Sugino and Oshiyama then studied electronic structure in a larger supercell of 216 atomic sites.

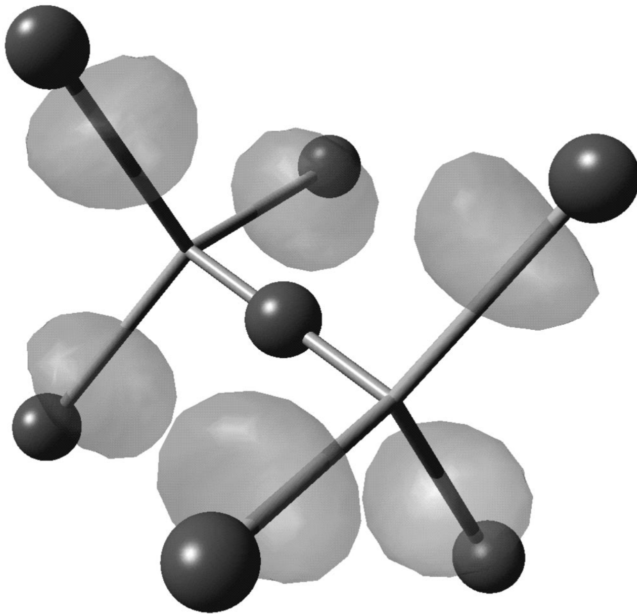

FIG. 2. Doubly negative Si vacancy. The spheres give the relaxed positions of the ions with respect to ideal bulk bonds denoted by sticks. The isosurface of the electron density for the highest deep level occupied by four electrons is also shown. The electron density for the isosurface is half of its maximum value of 0.087 electrons/Å^3.

They lowered the cutoff energy to 6 Ry so that the band gap opened to 1.1 eV. The density of the unpaired electron was found to be in a good agreement with ENDOR measurements.

The vacancy-formation energies defined with respect to the electric-chemical potential at the top of the valence band are also given in Table IV. It can be seen that the variations in the formation energy are largest for the doubly positive charge state and they become smaller towards the more negative charge states. Thus the trend is similar to that in the convergence of the magnitude of the lattice relaxation.

The ionization levels resulting from the total-energy calculations with different approximations are compared with experiment in Table V. The ionization levels between thermodynamically stable states are given in bold whereas those between a stable and an unstable one are shown in parentheses. The dashes mean that positive-charge states have not been found due to the hybridization of the highest occupied defect-induced state with the valence-band states. The negative-effective-U level (2+/0) is seen to converge nicely towards the experimental value when the size of the supercell increases. The experiments[4] indicate that the levels (0/−) and (−/2−) locate around the midgap and in the upper part of the gap, respectively. According to our calculations, the higher ionization levels could be close to or above the midgap, but the results are uncertain due to the too narrow LDA band gap of 0.47 eV. The Γ-point calculation with the 64-atomic-site supercell as well as with the largest supercell of 216 atomic sites give a second negative-effective-U level (0/2−), which is against the experimental findings. However, the relatively good convergence of the formation energies for the negative charge states in Table IV gives hope that the ionization levels calculated from them could be used as semiquantitative estimates. It is also noteworthy that the calculations using more extended **k**-point samplings as well as that with the 128-atomic-site supercell and the Γ point both give a thermodynamically stable singly negative charge state.

V. CONCLUSIONS

We have studied the convergence of electronic-structure supercell calculations for defects in semiconductors, with the vacancy in Si as the test case. The electronic structures have been described within the density-functional theory in the local-density approximation using norm-conserving pseudopotentials and a plane-wave expansion for the wave functions.

The convergence of the results is shown to be very slow. This is because the energy dispersion of the localized deep levels may lead for some choices of the Brillouin-zone sampling to hybridization of the defect state with the bulk-energy bands. If the supercell is not large enough the long-range ionic relaxation pattern, especially in the [110] zigzag direction, may not be properly described. The ensuing solutions may then have very different features, e.g., with respect to the point symmetry of the defect. The slow convergence of the supercell calculations should be borne in mind for different defects in semiconductors, although the vacancy in silicon may be one of the most difficult cases due to the flatness of the total-energy surface as a function of the ionic coordinates.

The calculations for the neutral vacancy in silicon show that the defect-formation energy can be estimated using

TABLE V. Ionization levels for the silicon vacancy. Numbers in the parentheses correspond to the transitions between a thermodynamically stable and an unstable charge state. The experimental results for the levels (2+/+) and (+/0) are from Ref. 4. All the values are in eV.

Size	(2+/+)	(2+/0)	(+/0)	(0/−)	(−/2−)	(0/2−)
64 & Γ	(0.50)	**0.43**	(0.35)	(0.70)	(0.59)	**0.65**
64 & Γ+L	(0.40)	**0.39**	(0.38)	**0.62**	**0.66**	(0.64)
64 & 2^3	–	–	–	**0.26**	**0.33**	(0.30)
64 & 3^3	–	–	**0.05**	**0.41**	**0.53**	(0.47)
128 & Γ	(0.32)	**0.28**	(0.24)	**0.39**	**0.52**	(0.64)
216 & Γ	(0.19)	**0.15**	(0.11)	(0.57)	(0.40)	**0.49**
EXPT.	(0.13)	**0.09**	(0.05)			–

small supercells with ~64 atomic sites, especially if **k**-point sets minimizing the effects of the defect-defect interactions are used. To conclude, the existence and position of different ionization levels is much more difficult. The too narrow LDA band gap also contributes to this difficulty. Finally, one has to be aware of the slow convergence when extracting structural information, such as the point symmetry to be compared with EPR data or the open volume of the defect to be compared with positron annihilation results.

Specifically, in the case of vacancy in silicon we have obtained the following (LDA) results, which have converged with respect to the size of the supercell and the **k**-point sampling of the Brillouin zone. The point symmetries for the doubly positive, singly positive, and the neutral charge state are T_d, D_{2d}, and D_{2d}, respectively. The nearest-neighbor atoms relax in all these charge states inwards, decreasing the open volume of the defect. The formation energy of the neutral vacancy is 3.3 eV. The ionization level (2+/0) lies 0.15 eV above the top of the valence band.

ACKNOWLEDGMENTS

This research has been supported by Academy of Finland through a MATRA grant. We also acknowledge the generous computer resources provided by the Center for the Scientific Computing (CSC), Espoo, Finland.

[1] See, for example, R. O. Jones and O. Gunnarsson, Rev. Mod. Phys. **61**, 689 (1989).

[2] See, for example, M. Scheffler, Adv. Solid State Phys. **22**, 115 (1982); O. Gunnarsson, O. Jepsen, and O. K. Andersen, Phys. Rev. B **27**, 7144 (1983); P. J. Braspenning, R. Zeller, A. Lodder, and P. H. Dederichs, *ibid.* **29**, 703 (1984).

[3] M. C. Payne, M. P. Teter, D. C. Allan, T. A. Arias, and J. D. Joannopoulos, Rev. Mod. Phys. **64**, 1045 (1992).

[4] For a review, see G. D. Watkins, in *Deep Centers in Semiconductors*, edited by S. T. Pantelides (Gordon and Breach, New York, 1986), p. 147.

[5] G. D. Watkins, in *Defects and Their Structure in Non-metallic Solids*, edited by B. Henderson and A. E. Hughes (Plenum, New York, 1976), p. 203.

[6] J. Mäkinen, P. Hautojärvi, and C. Corbel, J. Phys.: Condens. Matter **4**, 5137 (1992).

[7] G. A. Samara, Phys. Rev. B **37**, 8523 (1988); **39**, 12 764 (1989).

[8] G. A. Baraff, E. O. Kane, and M. Schlüter, Phys. Rev. B **21**, 5662 (1980).

[9] G. D. Watkins and J. R. Troxell, Phys. Rev. Lett. **44**, 593 (1980).

[10] M. Sprenger, S. H. Muller, and C. A. J. Ammerlaan, Physica B & C **116B**, 224 (1983); M. Sprenger, S. H. Muller, E. G. Sieverts, and C. A. J. Ammerlaan, Phys. Rev. B **35**, 1566 (1987).

[11] O. Sugino and A. Oshiyama, Phys. Rev. Lett. **68**, 1858 (1992).

[12] M. Scheffler, J. P. Vigneron, and G. B. Bachelet, Phys. Rev. B **31**, 6541 (1985).

[13] A. Antonelli and J. Bernholc, Phys. Rev. B **40**, 10 643 (1989).

[14] H. Seong and L. J. Lewis, Phys. Rev. B **53**, 9791 (1996).

[15] C. Z. Wang, C. T. Chan, and K. M. Ho, Phys. Rev. Lett. **66**, 189 (1991).

[16] S. Öğüt, H. Kim, and J. R. Chelikowsky, Phys. Rev. B **56**, R11 353 (1997).

[17] R. Virkkunen, M. Alatalo, M. J. Puska, and R. N. Nieminen, Comput. Mater. Sci. **1**, 151 (1993).

[18] L. J. Clarke, I. Štich, and M. C. Payne, Comput. Phys. Commun. **72**, 14 (1992).

[19] See Appendix A in S. Pöykkö, M. J. Puska, and R. M. Nieminen, Phys. Rev. B **57**, 12 174 (1998).

[20] L. Kleinman and D. M. Bylander, Phys. Rev. Lett. **48**, 1425 (1982).

[21] D. R. Hamann, Phys. Rev. B **40**, 2980 (1989).

[22] M. Fuchs and M. Scheffler, Comput. Phys. Commun. (to be published).

[23] S. G. Louie, S. Froyen, and M. L. Cohen, Phys. Rev. B **26**, 1738 (1982).

[24] X. Gonze, P. Käckell, and M. Scheffler, Phys. Rev. B **41**, 12 264 (1990).

[25] X. Gonze, R. Stumpf, and M. Scheffler, Phys. Rev. B **44**, 8503 (1991).

[26] D. M. Ceperley and B. J. Alder, Phys. Rev. Lett. **45**, 566 (1980); J. P. Perdew and A. Zunger, Phys. Rev. B **23**, 5048 (1981).

[27] N. Chetty, M. Weinert, T. S. Rahman, and J. W. Davenport, Phys. Rev. B **52**, 6313 (1995).

[28] D. Remler and P. A. Madden, Mol. Phys. **70**, 921 (1990).

[29] A. Baldereschi, Phys. Rev. B **7**, 5212 (1973).

[30] D. J. Chadi and M. L. Cohen, Phys. Rev. B **8**, 5747 (1973).

[31] H. J. Monkhorst and J. D. Pack, Phys. Rev. B **13**, 5188 (1976).

[32] S. Froyen, Phys. Rev. B **39**, 3168 (1989).

[33] G. Makov, R. Shah, and M. C. Payne, Phys. Rev. B **53**, 15 513 (1996).

[34] T. Korhonen, M. J. Puska, and R. M. Nieminen, Phys. Rev. B **54**, 15 016 (1996).

[35] D. J. Chadi, P. H. Citrin, C. H. Park, D. L. Adler, M. A. Marcus, and H.-J. Gossmann, Phys. Rev. Lett. **79**, 4834 (1997).

[36] A. Garcia and J. E. Northrup, Phys. Rev. Lett. **74**, 1131 (1995).

[37] S. Pöykkö, M. J. Puska, and R. M. Nieminen, Phys. Rev. B **53**, 3813 (1996).

[38] M. Pesola *et al.* (unpublished).

[39] P. E. Blöchl, E. Smargiassi, R. Car, D. B. Laks, W. Andreoni, and S. T. Pantelides, Phys. Rev. Lett. **70**, 2435 (1993).

[40] M. Ramamoorthy and S. T. Pantelides, Phys. Rev. Lett. **76**, 4753 (1996).

[41] O. Pankratov, H. Huang, T. Diaz de la Rubia, and C. Mailhiot, Phys. Rev. B **56**, 13 172 (1997).

[42] A. Zywietz, J. Furthmüller, and F. Bechstedt, Mater. Sci. Forum **258-263**, 653 (1997).

[43] G. D. Watkins and J. W. Corbett, Phys. Rev. **138**, A543 (1965); J. W. Corbett and G. D. Watkins, *ibid.* **138**, A555 (1965).